The Astrophysical Journal, 666:663–673, 2007 September 10

THE OPTICAL EXTRAGALACTIC BACKGROUND LIGHT: REVISIONS AND FURTHER COMMENTS

Rebecca A. Bernstein[1]

Received 2006 February 19; accepted 2007 April 30

ABSTRACT

We revise the measurements in our previous work of foreground zodiacal light (ZL) and diffuse Galactic light (DGL) that were used to measure the extragalactic background light (EBL). These changes result in a decrease of 8 and an increase of 0.3 in units of 10^{-9} ergs s^{-1} cm^{-2} sr^{-1} Å^{-1} ("cgs" units) in the ZL and DGL flux, respectively. We therefore obtain revised values for the EBL of 6 ± 4, 10 ± 5, and 7 ± 4 cgs in the *HST* WFPC2 U (F300W), V (F555W), and I (F814W) bands, respectively, from sources fainter than $m_V \sim 23$ AB mag. The revisions are dominated by the details of the tropospheric scattering models used to measure the ZL. We discuss these results in the context of faint number counts and diffuse EBL measurements at other wavelengths. In particular, we note that unless the slope of the galaxy counts increases beyond $m_V \sim 30$ AB mag, unresolved sources will contribute <0.2 cgs, which is far below the uncertainties achievable for any diffuse EBL measurement in the foreseeable future. Therefore, the best constraints on faint sources come from the resolved sources themselves. As in our earlier work, models are still required to derive the bolometric EBL (0.1–1000 μm) due to uncertainties in the mid-infrared; consequently, our previous discussions of the bolometric EBL are not affected by the revisions presented here. Finally, we discuss the nature of the extended point-spread function (PSF) of ground-based telescopes and its impact on surface brightness measurements. In particular, we show that the slope and amplitude of extended PSFs vary considerably between telescopes and with time. We find no conclusive, single cause of extended PSFs, although atmospheric scattering is ruled out.

Subject heading: diffuse radiation

Online material: color figure

1. INTRODUCTION

In a series of papers (Bernstein et al. 2002a, 2002b, 2002c, hereafter BFM02a, BFM02b, and BFM02c, respectively) we describe a measurement of the extragalactic background light (EBL) which was derived in two ways. The primary method was based on combining absolute photometry of the total flux of the night sky and of the individual foreground sources in one, $2' \times 2'$ *Hubble Space Telescope* (*HST*) WFPC2 field of view. The total background, $I_{\rm tot}$, was measured from space using *HST* WFPC2 in the F300W (U), F555W (V), and F814 (I) filters and using *HST* FOS (4000–7000 Å). The foregrounds include zodiacal light, $I_{\rm ZL}$, which was measured using ground-based spectrophotometry from the du Pont 2.5 m telescope at Las Campanas Observatory (LCO), and diffuse Galactic light, $I_{\rm DGL}$, which was estimated using a simple scattering model. The EBL was then identified by the simple relation

$$I_{\rm EBL} = I_{\rm tot} - I_{\rm ZL} - I_{\rm DGL}. \quad (1)$$

This method led to 1–2 σ detections of the EBL in all three bands. These flux levels were referred to as "EBL23" to indicate that they included only sources which are statistically well represented in the $2' \times 2'$ field of view of WFPC2, which are those sources fainter than $m_V = 23$ AB mag. The values of EBL23 measured in BFM02a were 4.0 ± 2.5, 2.7 ± 1.4, and 2.2 ± 1.0 in units of 10^{-9} ergs s^{-1} cm^{-2} sr^{-1} Å^{-1} (henceforth abbreviated as "cgs").

A second method was used to identify a *minimum* value for EBL23 based on the flux recovered from resolved sources in the *HST* WFPC2 images. To identify this minimum for EBL23, we used a technique that we called "ensemble photometry" in which the total flux surrounding detected objects in our *HST* images was extracted relative to the mean background level in the frame. This method allowed us to recover a significantly larger fraction of the total flux from the resolved sources than is recovered by standard Kron-like or aperture photometry using locally estimated values of "sky" for each object. This effect was confirmed and similar aperture corrections were found in *HST* ACS data (Benitez et al. 2004). Our final results for EBL23 were then the combination of these minima for EBL23 and the 1–2 σ measurements of EBL23 from absolute surface (spectro)photometry of the total background and foregrounds (see Table 10 of BFM02a).

Mattila (2003) has raised concerns regarding the estimates of $I_{\rm ZL}$ and $I_{\rm DGL}$ in our primary measurements of EBL23. We have discussed some of these in Bernstein et al. (2005, hereafter BFM05) and found that a net decrease in our $I_{\rm ZL}$ estimate of 0.5 ± 0.6 cgs was necessary, primarily due to changes in the zodiacal light (ZL) flux between the dates of our ground-based and *HST* observations (2–4 days). In this paper, we revise our estimates of the EBL as appropriate following a thorough discussion of our foreground measurements. We include here all of the concerns raised by Mattila (2003) and other issues regarding scattering and systematic uncertainties. We discuss the interpretation of these results in combination with the bolometric EBL at UV to IR wavelengths and the minimum values of the EBL derived from galaxy counts in BFM02a and other sources in the literature. All of the changes discussed here and in BFM05 are summarized in Tables 2 and 3.

2. MODEL FOR $I_{\rm DGL}$

In BFM02a, the contribution of diffuse Galactic light to the total background flux of our target field observed from *HST* (Galactic coordinates $l = 206.654^\circ$, $b = -59.767^\circ$) was estimated using a simple scattering model from Jura (1979),

$$I_{\rm DGL} = j_\lambda \omega_\lambda \tau_\lambda \left(1 - 1.1 g \sqrt{\sin b}\right), \quad (2)$$

[1] Astronomy Department, University of Michigan, Ann Arbor, MI, 48109.

in which ω is the albedo, g is the phase function of interstellar dust, τ is extinction, b is Galactic latitude, and j is the source function of the interstellar radiation field in the local solar neighborhood. The term in parenthesis in equation (2) reproduces the decrease in scattered light with increasing Galactic latitude, $|b|$, that results from the fact that scattering is preferentially forward and the integrated starlight (ISL) drops with increasing latitude. In BFM02a, τ_λ was derived from the value of the 100 μm flux in the *IRAS* 100 μm all-sky maps in our target field. This can be converted to extinction using the empirical scalings for 100 μm/N(H I) and N(H I)/A_λ, where N(H I) is the neutral hydrogen column density and A_λ is the extinction in magnitudes ($A_\lambda = 1.086\tau_\lambda$). As described in BFM02a, diffuse Galactic light (DGL) values were also increased slightly over the predictions of the Jura model to account for empirical colors of Galactic cirrus clouds found by Guhathakurta & Tyson (1989).

For reference, the DGL estimate in BFM02a was obtained as follows. We used $N(\mathrm{H\ I}) = 0.47 \times 10^{20}$ cm^{-2} for the total Galactic column density of H I, based on the 100 μm flux in the *IRAS* 100 μm all-sky maps and the scaling relation 100 μm/N(H I) derived from those data (Beichman et al. 1986). This was converted to $A(V) = 0.024$ mag using the extinction per H I column from Savage & Mathis (1979), which is consistent with $N(\mathrm{H\ I})/E(B-V) = 50 \times 10^{20}$ cm^{-2} mag^{-1}. The corresponding value for the DGL is 0.7 cgs at V based on the Jura model (eq. [2]). Including a 10% correction to compensate for the empirical colors of Galactic cirrus clouds, the estimated DGL at V was 0.8 cgs. The uncertainty was estimated to be (+0.5, −0.25) cgs.

As we noted in BFM02a, the *IRAS* maps are not accurately calibrated on an absolute scale. More accurate estimates of the 100 μm flux and hence N(H I) and A_λ might be expected from the recalibration of those maps by Schlegel et al. (1998, hereafter SFD98), as suggested by Mattila (2003); however, Schlegel et al. emphasize that at very low flux levels the relationship between 100 μm flux and N(H I) or A_λ is empirically variable in their maps by a factor of ~3. This is largely due to the difficulty of subtracting foreground ZL (and the EBL), which leads to zero-point uncertainties. At these levels, SFD98 note that their estimates of extinction may have comparable accuracy to the Burstein & Heiles (1982, hereafter BH82) estimates. It is not evident, therefore, that SFD98 (or any 100 μm surface brightness measurement) is the best source for identifying A_λ in our field. We therefore compare here five alternative estimates.

We can start by using the Jura model with alternative sources for the value of $A(V)$. There are at least three possibilities. First, despite the calibration caveats discussed above, SFD98 find $A(V) = 0.054$ mag for our field from their recalibration of the *IRAS* maps.[2] Second, the N(H I) column density as identified by 21 cm emission is 0.56×10^{20} cm^{-2} from BH82, corresponding to $A(V) = 0.022$ mag. Third, the N(H I) column density from the Leiden/Dwingeloo survey (Hartmann & Burton 1997, hereafter HB97) is 1.8×10^{20} cm^{-2} (99 K km s^{-1}), corresponding to $A(V) = 0.070$ mag. Using the Jura model, these three values of $A(V)$ give 1.8, 0.7, and 2.3 cgs for I_{DGL} in our target field.

Two other estimates of the optical DGL can be obtained from simple scaling laws identified in the *Pioneer 10* data (Toller 1981; reprinted in Leinert et al. 1998). The first is the rough, empirical relationship DGL = $N(\mathrm{H\ I})/(2.4 \times 10^{20}$ cm$^{-2})$, where DGL is then in $S_{10\,\odot}$ units.[3] This estimate is particularly rough since it ignores variations in the intensity of incident starlight over the sky. Using the range of N(H I) values from SFD98, BH82, and HB97, this corresponds to DGL fluxes of 0.7, 0.3, and 0.9 cgs, which lead to an average of 0.6 cgs. The second empirical scaling relation is the mean ratio DGL/ISL as a function of latitude at 4400 Å, which is 0.12 ± 0.02 at $b = |60\text{–}90|$. The mean value of the ISL within 5° of our field from Toller (1981) is 30.5 $S_{10\,\odot}$ (=36.3 cgs at 4400 Å). The DGL is then 4.35 cgs. This estimate ignores variations in dust column density with latitude, which is ~35% lower in our field than the mean at $b = |60|$ as measured by SFD98 or HB97. Adjusting for this lower column density, the corresponding DGL would be 2.8 cgs (=$0.12 \times 0.65 \times 36.3$ cgs).

The mean value of the five values derived above (1.8, 0.7, 2.3, 0.6, and 2.8) is 1.6 ± 1 cgs at V, where we adopt the full standard deviation as the uncertainty rather than the error in the mean to be conservative. As this source is included in the night-sky spectrum taken at LCO, it did contribute to the measured value of the diffuse ZL at the level of $I_{\mathrm{DGL}} e^{-\tau\chi} = 1.3$ cgs using the mean values of τ (0.19 mag per air mass) and χ (1.2 air masses) of our observations (see eq. [4]). As the DGL has Fraunhofer lines which are roughly 0.35 times as strong as the ZL (see § 3 and discussions in BFM02b and BFM05), roughly 0.5 cgs from the DGL was included in the measurement of I_{ZL} and was therefore subtracted from the *HST* measurement of I_{tot} in BFM02a (see eq. [1]). The remaining flux from I_{DGL} which should have been subtracted from I_{tot} was then $1.6 - 0.5 = 1.1 \pm 1$ cgs. This adjustment is included in our revised estimate of the EBL and included in the summary presented in Table 3.

3. MEASUREMENT OF I_{ZL}

The ZL was measured using spectrophotometry obtained from the du Pont telescope at Las Campanas Observatory. These are the only data that were obtained from the ground in our measurement of the EBL23. This complicates the measurement of the ZL and EBL23 in two ways. First, the ZL and total night-sky measurements must be calibrated onto the same absolute scale before subtracting one from the other, as discussed in BFM02a and BFM02b. For surface (spectro)photometry, such as of the EBL23 or ZL, flux calibration requires combining the usual flux calibration from point-source observations with an aperture correction that compensates for the light which is lost outside the photometric aperture or spectroscopic slit during point-source observations. This aperture correction is necessary because no analogous loss occurs in measuring the flux per unit solid angle from an extended source. In § 3.1, we consider additional evidence from the literature and additional data from the du Pont telescope to reexamine our treatment of this correction.

The second complication in measuring the ZL from the ground is due to the earth's atmosphere. The atmosphere influences the ground-based data in three ways: atmospheric extinction (scattering and absorption of light in the target field out of the beam), atmospheric scattering (light from the visible hemisphere of the sky which is scattered into the beam), and airglow emission. The observed night-sky spectrum from the ground can therefore be described as a function of wavelength (λ), time (t), air mass (χ), and atmospheric extinction (τ_{obs}) as follows (eq. [3] of BFM02b):

$$I_{\mathrm{NS}}(\lambda, t, \chi) = I_{\mathrm{target}}(\lambda) e^{-\tau_{\mathrm{obs}}(\lambda)\chi} + I_{\mathrm{scat}}(\lambda, t, \chi) + I_{\mathrm{air}}(\lambda, t, \chi), \quad (3)$$

where $I_{\mathrm{target}}(\lambda)$ is the sum of the diffuse sources in the target field, $I_{\mathrm{EBL}}(\lambda) + I_{\mathrm{ZL}}(\lambda) + I_{\mathrm{DGL}}(\lambda)$. To measure the zodiacal light, we utilized the fact that the zodiacal light is known to have a slightly

[2] Note that SFD98 use a conversion factor $N(\mathrm{H\ I})/E(B-V) = 80 \times 10^{20}$ cm^{-2} mag^{-1} and $A(V)/E(B-V) = 3.3$, which we adopt in all the calculations presented in this paper.

[3] 1 $S_{10\,\odot} = 1.18$ and 1.19 cgs at V and B, respectively.

reddened, solar-type spectrum with solar-strength Fraunhofer lines, and so can be expressed as a wavelength-dependent scaling times a fiducial solar spectrum, $C(\lambda)I_{\odot}$, in which $C(\lambda)$ is roughly linear. (See BFM02b, Leinert et al. [1998], and references therein for further discussion.) The airglow spectrum does not contain Fraunhofer features. We therefore identified the ZL flux by identifying the scaling factor $C(\lambda)$ that produces an airglow spectrum that has the minimum correlation with the solar spectrum, where $I_{\rm air}$ is then

$$I_{\rm air}(\lambda,t,\chi) = I_{\rm NS}(\lambda,t,\chi) - I_{\rm ZL}\left\{e^{-\tau_{\rm obs}(\lambda)\chi} + \left[\frac{I_{\rm EBL}(\lambda)+I_{\rm DGL}(\lambda)}{I_{\rm ZL}}\right]e^{-\tau_{\rm obs}(\lambda)\chi} + \frac{I_{\rm scat}(\lambda,t,\chi)}{I_{\rm ZL}}\right\}. \quad (4)$$

The scattering term $I_{\rm scat}$ is identified by modeling atmospheric scattering from all sources that include Fraunhofer lines: the interstellar light (ISL), diffuse Galactic light (DGL, see below), and zodiacal light (ZL) itself. Note that the ISL and DGL contain a mixture of stellar types and therefore have Fraunhofer lines which are roughly 0.35 times as strong as in the ZL on average (see Figs. 29 and 30 of BFM02b). To remove the absolute flux of ZL from the models of scattered light, we express the scattered ZL as a fraction of the ZL in the target field, as implied by equation (4). This leaves the relative strength of the ZL over the sky but not the absolute value as a source of uncertainty in the scattering models.

There are several changes which should be made to the measurement of the ZL in BFM02b by this technique. First, the EBL and DGL terms in equation (4) were dropped from the analysis in BFM02b because they were not expected to have Fraunhofer features. This is correct for the EBL, but the DGL can contribute Fraunhofer features, as mentioned above, and so should be included as a contributor in the target field (done in § 2, above) and as a source of scattering. Second, the scattering models used to identify $I_{\rm scat}$ are complicated and involve a number of parameters, secondary effects, and uncertainties which we estimated and documented in BFM02b. Mattila (2003) has suggested alternate values and treatments for several of these, and we consider his comments and other ideas here and incorporate the changes where appropriate. We include estimates of the change in the scattered light models in each section and summarize these in Table 2. These estimates are calculated at the mean air mass ($\chi = 1.2$), wavelength ($\lambda =$ 4600 Å), and atmospheric extinction [$\tau(4600\ \text{Å}) = 0.19$ mag per air mass] of all the spectra used in our measurement of $I_{\rm ZL}$.

The individual estimates and net change to the ZL that are discussed here have all been confirmed explicitly using the scattering models and fitting methods used in BFM02b and BFM05. The changes are discussed here qualitatively and quantitatively so that the sense and magnitude of the changes and the uncertainties may be fully appreciated.

3.1. *Aperture Corrections*

For the *HST* data, the aperture correction we applied is from Holtzman et al. (1995) and accounts for flux at 0.5″–6.0″, beyond which no significant flux from point sources is identified (see references and discussion in Holtzman et al. and BFM02a). To calibrate the LCO spectra, spectrophotometric standards were observed through a slit 10.8″ wide. To measure the aperture correction relevant to these data, we used direct imaging data taken on the last night of the 1995 observing run to measure the point-spread function (PSF) from 5.4″ to 25″ in radius. We found the flux in that annulus to be 2.1% ± 0.2%. We therefore applied an aperture correction of 0.979 to compensate for this lost light.[4] The concern has been raised by Mattila (2003) that the aperture correction for our ground-based spectroscopy should have been derived from the PSF over a much larger range in radius. This concern is based, first, on the theory that the surface brightness of the extended PSF of a star will always follow an inverse-square law with radius over several degrees (e.g., King 1971) and, second, on the belief that the full profile is due to scattering by the optics of the telescope, specifically mirror microripple and collected dust. This second point is critical, because if the extended profile is not due to the telescope itself then a correction should not be applied. If, for example, the profile is due to the atmosphere (i.e., atmospheric scattering), then it is compensated explicitly through atmospheric extinction corrections that are already made as a standard part of point-source calibration techniques; if it is due to optical elements that are in the optical path only during imaging (i.e., filters, dewar windows, reimaging optics, etc.) then it is also not appropriate for a spectroscopic measurement in which the only optics between the spectrograph slit and the sky are the primary and second mirrors of the telescope. Here we therefore discuss both the theoretical understanding of the extended PSF and new, direct measurements of the PSF of the du Pont telescope in direct imaging mode.

Measurements of the large-angle PSF exist in the literature for many telescopes and observatories (see Table 1). While it is true that a global feature of these measurements is a power-law relation between surface brightness (μ) and radius (r) at $r > 10''$ ($\mu \propto r^{\alpha}$), the exact value of α and the total flux in the extended halo varies considerably, so that the flux beyond 25″ is not well predicted. The original King (1971) measurement was made using Palomar Observatory Sky Survey blue plates and followed an r^{-2} profile at 30″–1°. This was consistent with the profile measured by de Vaucouleurs (1958) in the *B* band using the Lowell Observatory 21 inch reflector, 4.5 years after its last aluminization (i.e., with significant dust accumulation).[5] Using the same telescope and plate photometry taken between 1971 August and 1972 April, Kormandy (1973) found a similar profile with $\alpha = -2$ at 10″–3′ (modulo a ghost at 1′), but $\alpha = -1.7$ at 3′–30′. Also using the same telescope between 1971 March and April, Shectman (1974) found a PSF slightly (25%) brighter than King (1971) found at 100″ and a much steeper slope of $\alpha = -2.6$ (although the slope is mistakenly identified as $\alpha = -2$ in the text of that paper). Thus, the PSF of even this one telescope is not well determined within a time frame of even a few months. In this case, the variations are probably a result of differences between filters, emulsions, and mirror cleanliness, as discussed below, and possibly measurement errors.

Other results in the literature, summarized in Table 1, vary by factors of 0.6–1.7 relative to the King profile at 10″–30″ and follow power laws with $-3 < \alpha < -1.7$. The measurements in Table 1 were made at a wide range of sites and wavelengths (*B* to *R* band), with a wide range of instruments, and with mirror coatings ranging from fresh (clean and uncorroded) to 4.5 years old.

[4] A second aperture correction was applied to account for scattered light in the spectrograph which is missed when the spectra of standard stars are extracted. This second aperture correction was 0.984. The total correction applied was then $0.984 \times 0.979 = 0.963$. Only the correction for light lost in the focal plane is being remeasured here.

[5] It is worth noting that the claim of having measured the profile out to 1° or more is suspect because the measurements discussed by de Vaucouleurs (1958) targeted Jupiter and were based on scans "north and south," which would be sufficiently orthogonal to the zodiacal plane that the "sky" level (more than 50% zodiacal light) would have varied by more than the source halo over degree scales, as would the surface brightness of then-unknown Galactic cirrus.

TABLE 1
PSF Measurements

Reference	Observatory	Telescope	Altitude (m)	Bandpass	PSF	
					μ[a] (mag arcsec^{-2})	α
King (1971)[b]	Palomar	48 inch Schmidt	1713	B	12.7 at 10″, 15.0 at 30″	−2 at 10″–30′
Kormandy (1973)	Palomar	48 inch Schmidt	1713	B	1 × King at 30″	−2 at $r < 3'$, −1.7 at $r > 3'$
Shectman (1974)	Palomar	48 inch Schmidt	1713	RG-1	1.25 × King at 100″	−2.6
Capaccioli & de Vaucouleurs (1983)	McDonald	0.9 m	2100	B	0.6 × King at 10″	(−1.6, −1.8) at $r > 10''$
Middlemass et al. (1989)	La Palma	2.5 m	2325	6563 Å	2 × King at 10″	−3.5 at 10″–25″
Surma et al. (1990)[c]	Calar Alto	1.23 m	2190	R	4.8 × King at 10″, 1.4 × at 30″	−1.6 at 30″–100″, −2.0 at 100″–300″
Uson et al. (1991)	KPNO	No. 1 0.9 m	2160	R	1.6 × King at 30″	−2 at 30″–800″
Mackie (1992)	KPNO	Burrel 0.6 m	2160	g	1.7 × King at 20″	−2 at 20″–100″
Gonzalez et al. (2005)	LCO	Swope 40 inch	2282	i	[d]	−1.6 at 10″–40″, −2.2 at 40″–400″
This work	LCO	du Pont 2.5 m	2282	r	1.2 × King	(−2.5, −3) at 10″–400″

[a] Surface brightness for a star normalized to 0 mag and based on the fit to the measured profile.
[b] The measured surface brightness shows scatter of roughly 1 mag arcsec^{-2} around the fit.
[c] This measurement was made using a reimager, which means that the PSF includes the scattering and ghosting properties of a multielement optical system in addition to the telescope and atmosphere. It is included here for completeness but is not comparable with direct imaging through a reflective telescope.
[d] The value of μ is not given.

The wide range of results in Table 1 obviously demonstrates that an r^{-2} PSF should not be considered typical and that, moreover, there has never been evidence for a "standard King" profile.

For the purpose of comparing surface brightness measurements between telescopes, as is our goal, it is also critical to understand whether the source of the PSF is the atmosphere, the telescope (primary and secondary mirrors, in the case of the du Pont), or the instruments beyond the secondary mirror. First, it is highly unlikely that atmospheric scattering is a significant contributor to any PSF which falls off even as sharply as r^{-2} because both Rayleigh and Mie scattering in the atmosphere fall off much more gradually with angular distance (see § 3.2 and BFM02b). This leaves the telescopes (including mirror microripple, dust, and the aluminization coating itself) and optical elements near the focal plane during imaging, including any reimaging optics that may be present, filters, dewar windows, emulsions, glass plates, and the CCD itself. Any surfaces in the optical path can contribute to the PSF as a result of double-bounces between any two surfaces. The PSF will clearly depend on the telescope and instrumental setup.

Regarding the likely contributions from the telescope optics, Mattila (2003) points out that Beckers (1995) suggests the following surface brightnesses at radii of 1″, 10″, and 100″:

1. 8.7, 16.2, and 23.7 due to diffraction on telescope aperture ($\mu \propto r^{-3}$);
2. 10.3, 15.3, and 20.3 due to mirror microripple ($\mu \propto r^{-2}$);
3. 10.5, 15.5, and 20.5 due to dust ($\mu \propto r^{-2}$).

These values are for a 0 mag star in 0.7″ seeing on an 8 m telescope and, while they are not justified by Beckers (1995) in those conference proceedings, they are typical of discussions in the adaptive optics literature pertaining to infrared wavelengths (see summaries in Racine 1996 and Beckers 1993). Diffraction scales with the inverse of telescope diameter, so that scattering will be brighter at the same angles by about 1.25 mag arcsec^{-2} on the 2.5 m du Pont. The combined surface brightness of the PSF from these estimates would then be about 14 and 19.5 mag arcsec^{-2} at 10″ and 100″, respectively.

To better understand these estimates, we can compare them with some simple approximations. Mirror microripple can be approximated using a robust formula derived by Stover (1990) for the total integrated scatter (TIS) from a surface with "microripple" roughness with rms amplitude σ: TIS $= (4\pi\sigma/\lambda)^2$. A typical-quality mirror has microripples with rms amplitude of 1 nm and length scales (l) of 1 mm (S. Shectman 2004, private communication), giving TIS $\sim 0.1\%$. The total integrated scatter from the primary and secondary mirrors together is then 0.2% for typical-quality mirrors. This is much smaller than the estimate from Beckers (1995). The characteristic scattering angle is given by the slope of the ripples, σ/l, and so would be $\sim$0.2″ for a typical-quality mirror, which is also much smaller than Beckers (1995) suggests.

The total accumulation of dust with time can be estimated from the fact that a 20% drop in reflectivity is typical of a primary mirror's performance at LCO with one year's worth of dust accumulation (F. Perez 2004, private communication). For dust particles with a size distribution larger than $\sim$1 μm, scattering will be preferentially forward (toward the dusty mirror) for optical light. If the dust albedo is around 8%, as for "dirt" at LCO (see § 3.2.2), then a mirror with enough dust to cause a 20% drop in reflectivity could have a dust scattering contribution of $\sim$1.6%. The estimate from Beckers has a total flux of 0.5%, which might be reasonable for a mirror in an "average" state—a few months after aluminizing or cleaning. Little dust accumulates on secondary mirrors since they point down, so the expected effect of dust is something less than 1.5% scattering due to dust one year after washing.

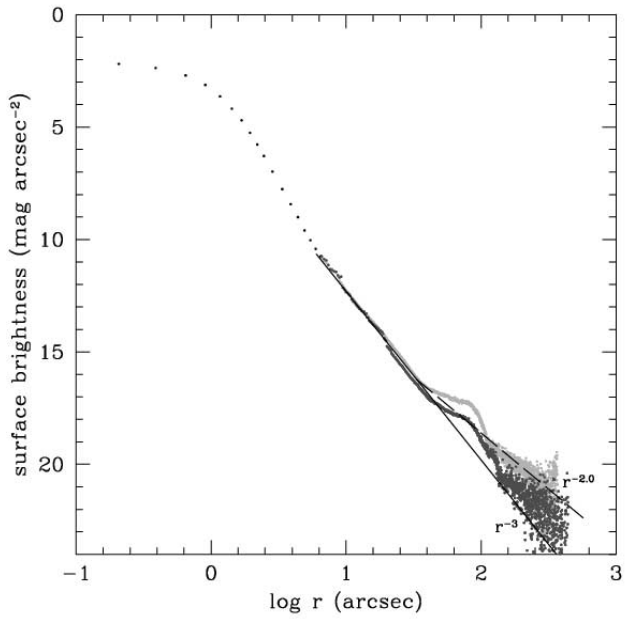

FIG. 1.—PSF of the du Pont 100 inch telescope based on data taken in 1998 August with the star centered in the image (*light gray points*) and in 2000 September with the star $\sim$3′ off-axis in the image (*dark gray points*). Surface brightness is in units of mag arcsec^{-2} for a star with total flux normalized to 0 mag. The bump at $60'' < r < 100''$ ($1.6 < \log r < 2$) seems to be caused by a reflection near the focal plane (between the CCD and the dewar window or filter), as it does not appear in the profile of stars which are off the edge of the detector.

It appears that a wide range of PSF amplitudes and slopes can be predicted from theoretical arguments and empirical evidence, and that there is no "standard" PSF. It therefore seems clear that the PSF must be measured directly on any specific telescope to be relevant. For the aperture correction measured in BFM02b, we used direct imaging data taken during our 1995 observing run. In those data, we found the PSF to contain 2.1% ± 0.2% of the star's flux at 5.4″–25″. We have since measured the PSF out to 400″ in direct imaging data obtained in 1998 August and 2000 September using the same filter and detector both years. The 1998 and 2000 data were taken for the purpose of measuring diffuse light in clusters and have 1 σ flat-fielding uncertainties of 0.06% of the sky flux ($\sim$29.5 mag arcsec^{-2}) on scales from one seeing disk to the full image diameter (1″–8′; Krick et al. 2005). Using these data, we have measured the PSF at $1'' < r < 400''$ (see Fig. 1). We find that it is fairly stable between runs over scales $1'' < r < 40''$ ($\log r < 1.6$) and contains 2.4% of the star's light at 5.4″–25″. If the flux at 5.4″–25″ were being measured relative to the "sky" surface brightness in an annulus at 25″–30″ as in BFM02b, rather than relative to the sky measured at >1000″ as is possible in these data, then we would find 2.3% of the star's light at 5.4″–25″. The PSF in the 1995, 1998, and 2000 data all appear to be consistent on *scales less than an arcminute*.

During the 1998 and 2000 runs, stars were imaged in a range of locations—on-axis, off-axis but near the edge of the image, and completely off the edge of the detector by up to many arcminutes. In Figure 1, we have plotted the profile for a star which was well centered (the 1998 profile) and for a star which was 3′ off-axis (the 2000 profile). There are two differences between the profiles for on- and off-axis stars. The first is the location and

TABLE 2
CORRECTIONS TO I_{ZL}

Correction	BFM02	Current	Change	Term Affected	ΔI_{EBL} (4600 Å) (cgs)
Corrections from BFM05	...	...	$-0.005\% \pm 0.006\%$	I_{ZL}	$+0.5 \pm 0.6$
ZL calibration[a] at $r > 25''$ (§ 3.1)	$2.1\% \pm 0.2\%$	3.6 ± 1	$1.5\% \pm 1\%$	I_{ZL}	$+1.5 \pm 1$
Scattering model:					
Particulate albedo (§ 3.2.1)	0.59	0.94	-3.4 cgs	I_{ZL}	$+3.4 \pm 0.5$
Ground reflectance (ZL) (§ 3.2.2)	...	7%–14%	-1.5 ± 1 cgs	I_{ZL}	$+1.5 \pm 1$
DGL as scattering source (§ 3.2.3)	...	See § 3.2.3	-1.4 ± 0.3 cgs	I_{ZL}	$+1.4 \pm 0.3$
Uncertainty in models (§ 3.2.4)	...	...	...	I_{ZL}	± 3
Uncertainty in scattering sources (§ 3.2.4)	...	...	...	I_{ZL}	± 2
Net change	...	...	...	...	-8 ± 4

[a] Aperture correction.

magnitude of the bump at $60'' < r < 100''$, which is probably caused by a reflection near the focal plane (between the CCD and the dewar window or filter), as it does not appear in the profile of stars which are off the edge of the CCD. Note also that this reflection between the CCD and dewar *could not occur* during spectroscopy when there is only a slit plate in the focal plane of the telescope and no opportunity for a double reflection. It is therefore clear that this feature should not be included in our estimate of the PSF of the telescope. The second difference is the slope of the PSF at $r > 100''$, which seems to differ somewhat from the slope at $r < 40''$. To the limit of the measured profiles in both data sets (400″), the halo profile has $-2 < \alpha < -3$, depending on the range of r over which we fit the profile, how we include the "bump" feature at 60″–100″, and the uncertainty in the sky estimate.

To compare with the predicted scattering angles and total scattered light due to microripple and dust, discussed above, we note first that the du Pont mirror was washed or aluminized roughly 2–3 months before our 1998 and 2000 observing runs (used to measure the PSF here) and 9 months before the 1995 run (used to measure I_{ZL} for BFM02a).[6] Based on both the Beckers estimates and our own estimates above, the scattered light we measure in 1998 and 2000 (with only 2–3 months accumulated dust) is larger than one would anticipate from dust and microripple. We also note that the PSF we measure at 5.4″–25″ (small angles) is relatively stable between all three runs, despite the probable difference in likely dust accumulation. The dominant cause of the PSF is therefore probably neither dust nor microripple. It is possible that a significant contribution comes from scattering due to the filter (multilayer dielectric coatings on glass substrates) and antireflection coatings (also multilayer dielectric coatings) on the filter, dewar window, or CCD. Regardless, the empirically measured PSF of the du Pont has a fairly stable amplitude and profile, particularly if the optical effects associated with the imager (such as the bump) are removed.

In an effort to be conservative about the uncertainties, we estimate a lower and upper limit to the flux in the halo for a reasonable range of power laws out to 1°. While none of the measurements in the literature give compelling empirical evidence for a stellar profile with a constant power-law slope (due to the telescope) that extends to a degree, much less "infinity," the additional flux beyond 1° is insignificant compared to the uncertainties for any reasonable profile. The integrated flux in the two halos measured and plotted in Figure 1 at 25″–400″ is 1.0% and 1.5%. One might reasonably regard these as *upper* limits, given that the reflections responsible for the bump feature are certainly not present in a spectroscopic measurement. For comparison, the integrated flux at 25″–3600″ is 2% for an r^{-2} profile and roughly 0.4% for an r^{-3} profile. To be conservative, we adopt a value for the extended PSF beyond 25″ of $1.2\% \pm 1\%$. Combined with the PSF at 5.4″–25″ (2.4%), the total aperture correction should be $3.6\% \pm 1\%$. We include this change in Table 2.

[6] The primary mirror of the 100 inch telescope at LCO was aluminized on 1994 January 21, 1996 January 8, 1998 May 6, and 2000 July 14. It was washed in January of 1995, 1997, and 1999.

3.2. *Scattering Models*

When observed from below the atmosphere, a source will appear fainter due to extinction (absorption and scattering) along the line of sight. Atmospheric extinction is dominated by Rayleigh scattering (due to molecules), which has a phase function proportional to $1 + \cos^2\theta$, where θ is the scattering angle relative to incidence. Roughly one-fourth of the extinction is Mie scattering (due to particulates), which has a forward-peaked, narrow phase function and drops by roughly a factor of 10 between 0° and 10° and by a factor of several hundred by 50°. The particulate albedo is large, so that little of the extinction is due to absorption.

For an extended source which covers a large fraction of the sky, such as the zodiacal light, light will also scatter *into* the line of sight from all over the visible hemisphere of the sky. For the purposes of our ZL measurement from LCO, any source which will have spectral features in common with the zodiacal light in our field of view is of concern as a source of scattered light. The scattered light coming into the field of view from any source is included in equations (3) and (4) as I_{scat}. This scattering can be modeled by integrating the scattering contribution from each volume in the beam along the line of sight from the telescope to the top of the atmosphere. Every volume in the beam will receive light from all over the visible hemisphere of the sky. This calculation was described in BFM02b. In BFM02b, the sources considered for that scattered light were zodiacal light and integrated starlight (ISL). Mattila (2003) has pointed out three changes that should be made to our scattering calculations: the particulate albedo value should be increased; ground scattering should be included; and the DGL, which has an ISL-like spectrum, should be included as a scattering source. We discuss these and other details of the scattering models in the following sections.

3.2.1. *Particulate Albedo*

The extinction caused by atmospheric molecules is due to scattering, while the extinction due to particulates is also partly due to absorption. The albedo adopted for aerosol particles in BFM02b was 0.59, following the discussion in Staude (1975) for "dry"

air. A more accurate value for optical wavelengths is roughly 0.94 (McClatchey et al. 1978, Table 6), independent of altitude. The Mie-scattered ZL and ISL in BFM02b should increase by a factor of 1.6 with this change. At 4600 Å and $\chi = 1.2$, Mie-scattered ZL in BFM02b is $\sim 0.04 I_{\rm ZL}$ and therefore should be increased by $0.024 I_{\rm ZL}$, or 2.6 cgs. The Mie-scattered ISL in BFM02b is ~3.7 cgs, and so should be increased by 2.2 cgs; because the Fraunhofer lines are 35% as strong in the ISL as in the ZL, the ZL measurement is affected at the level $2.2 \times 0.35 = 0.8$ cgs due to the ISL. The total correction due to Mie-scattered ZL and ISL is 3.4 cgs. If the particulate albedo from McClatchey et al. (1978) is uncertain by 10%, corresponding to albedo values between 0.85 and 1.0, then the uncertainty in the ZL due to the Mie-scattered ZL and ISL is ±0.5 cgs.

3.2.2. *Ground Reflectance*

Any light which hits the ground can be reflected up, and subsequently scatter back down again into the line of slight. As Mie scattering is strongly forward, only Rayleigh scattering contributes significantly to this second scattering event. Ground reflectance is generally between 2% for vegetation and 8% for dry soil (McClatchey et al. 1978). The contribution due to ground reflectance can be estimated by assuming that 80% ($e^{-\tau\chi}$, with $\tau \sim 0.2$ and $\chi \sim 1$) of the light from above the atmosphere hits the ground, at most 8% is reflected back up, and at most 20% ($1 - e^{-\tau\chi}$) is scattered back down again: $0.8 \times 0.08 \times 0.20 = 0.01$. This is a conservative estimate for at least two reasons: the average value of χ over the sky is around 2.5, not 1, so that less light on average reaches the ground; and only a fraction of the second scattering event will send light back into the beam. Moreover, LCO is on a peak—the surrounding valleys are at an altitude of less than 4500 feet within even 0.5 miles of the telescopes and west of the observatory the altitude continues to fall all the way to sea level within ~100 km; this means that attenuation of light *below* the observatory will prevent all of the scattered light from reaching to above the altitude of the observatory (8200 feet) where our backscattering estimate would be relevant.[7] This is particularly true if there is an inversion layer near the altitude of the observatory, which there often is. Nevertheless, ground scattering does systematically contribute flux and should be included in our estimate of the net effect of atmospheric scattering. We can obtain a rough estimate of the ground scattering as follows below.

The relevant area for ground scattering around the telescope is small (~100 km × 100 km) because the scattering is exponentially stronger near the ground and the Rayleigh scattering phase function is proportional to the cosine squared of the angle, making larger distances irrelevant. The ground reflectance has been measured by the *MODIS* satellite and is publicly available for the years 2001 and 2002, as Mattila (2003) points out. The average reflectance for November of 2001 and 2002 is roughly 7% at the coordinates of Las Campanas (70.7° west longitude, −29.0° latitude). The surface reflectance increases to 8% going east 50 km and decreases to 5% going west 50 km, so that 7% is also a reasonable average value for the area around LCO. Another concern, however, is that there could have been some fog in the valleys at night. The relative humidity was 40%–50% and 30%–45% on 1995 November 25 and 27, respectively, and the wind was low (under 15 miles hr^{-1}) on both nights. These conditions are often accompanied by some low-density fog in the valleys. In that case, one might estimate that 10%–50% of the area within 100 km of the telescope was covered in the low-altitude regions immediately surrounding and to the west of the observatory. According to McCartney (1976), the scattering phase function for fog is strongly forward scattering for droplet sizes larger than the wavelength of light. Fog or cloud droplets, which have sizes in the range 1–10 μm, are modeled to have phase functions with total scattering at 90°–180° (backscattering) of about 1%–2% at optical wavelengths (McCartney 1976). However, multiple scattering events can result in an effective surface albedo for "dense" fog that is around 20% (Bendix et al. 2004). If up to 50% of the area around LCO was covered by low to moderate density fog, the very highest one might estimate for the ground reflectance is 14% (the average of 7% for no fog and 20% for dense fog). As explained above, this is an overestimate in several regards, so we consider it to be an upper limit.

The fractional contribution from ground reflectance as a function of zenith angle, extinction, and ground albedo has been modeled by Ashburn (1954, Table 1). The fractional contribution of ground scattering relative to the source flux varies with extinction and air mass in these models, but it is a fairly constant fraction of the atmospheric Rayleigh scattering for any value of the Rayleigh extinction. Interpolating from Ashburn's Table 1, ground scattering of 7% (or 14%) will increase the scattering by 0.06 (or 0.12) times the Rayleigh scattering in the atmosphere. However, those models do not assume that the observing sight is on a peak with a valley floor several thousand feet below and falling off to sea level. So again, we can assume that these models will overestimate the scattered light since the second scattering event that sends light down may occur below the altitude of the observatory. Nevertheless, at 4600 Å and $\chi = 1.2$, the Rayleigh scattering due to ZL is $0.15 I_{\rm ZL}$ and therefore the Ashburn models suggest that it should be increased by between $0.01 I_{\rm ZL}$ and $0.018 I_{\rm ZL}$ (=1–2 cgs) for a ground albedo of 7%–14%. The Rayleigh scattering component of the ISL is 9.5 cgs, and therefore increases by 0.6–1.1 cgs and will increase the observed ZL measurement by 0.35 times these values, or 0.2–0.4 cgs. The net correction for ground scattering is then between 1.2 (=1 + 0.2) cgs and 2.4 (=2 + 0.4) cgs. Again, this range is likely to be an overestimate, for the many reasons we discuss above. We adopt the value 1.5 ± 1 cgs and include this correction in Table 2.

3.2.3. *Scattered DGL*

As discussed above, the scattered DGL should scale with extinction and ISL along the line of sight. Empirically, Toller (1981) finds DGL/ISL ≈ 0.21, 0.34, 0.31, 0.19, 0.25, 0.17, 0.17, and 0.12 at absolute latitude ranges 0°–5°, 5°–10°, 10°–15°, 15°–20°, 20°–30°, 30°–40°, 40°–60°, and 60°–90°. It is clear from Toller's data (replotted in Leinert et al. 1998) that these scalings are rough, but they are surprisingly consistent at all latitudes with the mean values we obtain from the Jura (1979) model and the N(H I) maps discussed in § 2. We therefore expect them to be accurate to within a few percent, consistent with the quoted errors from Toller (1981). If we adopt these ratios, the net flux of the scattered DGL averaged over the visible hemisphere is roughly 0.25 ± 0.05 times the scattered ISL at all air masses and wavelengths. At 4600 Å and $\chi = 1.2$ the ISL is 15.6 cgs, including the corrections discussed in §§ 3.2.1 and 3.2.2. The total contribution from scattered DGL is then roughly 4.0 cgs, and so contributes 1.4 ± 0.3 cgs to the ZL, where the error is dominated by the uncertainty in the DGL model itself.

3.2.4. *Uncertainty in Scattering Models*

The accuracy of the scattered light estimates can be considered in terms of the accuracy of the scattering parameters (ground

[7] Atmospheric extinction is about 3 times greater at sea level than at 8000 feet (McClatchey et al. 1978).

TABLE 3
Revised EBL23 Results

Term in Equation (3)	BFM02			Current		
	F300W	F555W	F814W	F300W	F555W	F814W
I_{tot}	33.5 ± 2.5	105.7 ± 1.5	72.4 ± 1.0	33.5 ± 3.3	105.7 ± 2.3	72.4 ± 2.0
I_{DGL}	1.0 ± 0.5	0.8 ± 0.5	0.8 ± 0.5	1.1 ± 1	1.1 ± 1	1.1 ± 1
I_{ZL}	28.5 ± 0.4	102.2 ± 1.2	69.4 ± 0.9	26 ± 1	94 ± 4	64 ± 3
I_{EBL23}	4 ± 2.5	2.7 ± 1.4	2.2 ± 1.0	6 ± 4	10 ± 5	7 ± 4
Minimum EBL23	3.2 ± 0.22	0.89 ± 0.01	0.76 ± 0.01	...	...	...
I_{ground} ($m < 23$) AB mag	0.27 ± 0.05	0.49 ± 0.1	0.65 ± 0.13	...	...	...

scattering, particulate albedo, and observed atmospheric extinction), the absolute flux of the sources (DGL, ISL, and ZL), and the accuracy of the models themselves.

In the previous sections, we have discussed the accuracy of the scattering parameters as summarized in Table 2. The only scattering parameter not discussed explicitly above is the observed extinction coefficient. As discussed in BFM02b, the standard deviation in the combined sensitivity and extinction function derived from 15 standard stars was 0.011 mag. It is therefore very unlikely that the extinction solution is in error by more than 1%. Moreover, the extinction (scattering out of the line of sight) and the scattering into the line of sight increase or decrease together for small changes in the extinction, so that the net result of small errors in the extinction solution is negligible.

Regarding the scattering sources, if the ISL flux and DGL flux are in error by 10%, then the ZL changes by ±0.5 cgs. Uncertainties of 10% in the ZL around the sky relative to the flux in our target field change the estimated ZL by ∼1 cgs at the mean wavelength and air mass. These uncertainties were discussed in BFM02b. Added in quadrature, they impact the ZL measurement by about 2 cgs. This is listed in Table 2 for completeness.

Regarding to the accuracy of the scattering models themselves, Staude (1975) compared his scattering calculations with those of Ashburn (1954) and Wolstencroft & van Breda (1967), which we have followed here, and found the results to be consistent to within ±10% at zenith angles less than 70° assuming that all atmospheric and scattering parameters were well known. In BFM02b, we estimated that the uncertainty over smaller zenith angles (0°–60°) was ±8% based on that comparison. To be more conservative, we increase that estimate now to 10% (2–3 cgs). The only additional uncertainties not discussed above which might affect the scattering results are the scale height of the atmosphere and complications near the horizon associated with refraction and very large path lengths. The scale height at standard temperature (273 K) is 8.0 km and changes linearly with temperature. For a change of 15° (5%) the scale height also changes by 5% to about 8.4 km. This does not effect the net extinction or scattering, which is constrained by the observations of standard stars, and so has a negligible affect on the total scattered light. The same is true for the effect of the particulate scale height. Finally, the contribution of scattering from lines of sight within 5° of the horizon is subject to increased uncertainties because the total path length is sensitive to refraction effects and is difficult to properly calculate. The nominal contribution from these angles is roughly 1 cgs without taking refraction into account, and we adopt an uncertainty of 1 cgs. The total uncertainty in the scattering models is then about 3 cgs (see Table 2).

The combination of the uncertainties due to the mean flux of scattering sources over the sky as discussed in this section, the models themselves, and remaining items in Table 2 is 4 cgs, which is about 25% of the total scattered light contribution to the ZL measurement.

4. REVISED ESTIMATES OF EBL23

We have incorporated all of the corrections discussed here and in BFM05 to revise our EBL23 results. The corrections to the ZL measurement are summarized in Table 2. The individual components of the primary EBL23 measurement (see eq. [1]) are summarized in Table 3. To estimate the ZL flux in the *U* and *I* bands of WFPC2, we assume that the ZL is redder than the Sun by 5%/1000 Å, consistent with our own measurements (see *HST* FOS in BFM02a) and with measurements of the ZL from space, summarized in Leinert et al. (1998). These references can be consulted for further discussion of the ZL scattering and color.

The uncertainties pertaining to all issues discussed in this paper regarding the ZL measurement are listed and combined in § 3.2.4 and Table 2. Additional contributions from the data analysis discussed in BFM02b include the uncertainties in the solid angle of the observations (0.6%; see BFM02b, § 3.6.3), the point-source flux calibration (0.6%; see BFM02b, § 3.6.1), and the statistical uncertainty in the measurement of the Fraunhofer features (1%; see BFM02b, § 6). Finally, a 2.5% uncertainty should be included for the *U* and *I* bands to account for uncertainty in the color of the zodiacal light relative to the Sun (±1%/1000 Å; see Leinert et al. 1998). Combining these in quadrature gives 4.8% (1.3 cgs) in *U*, 4.2% (4.2 cgs) in *V*, and 4.8% (3.1 cgs) in *I*.

We note also that the estimated uncertainty of the *HST* WFPC2 point-source flux calibration has been revised from 1%–2% over the bands used here to 2% for the F555W and F814W bands and 3%–4% for the bluer bands (explicitly F336W and F439W; see Heyer et al. 2004). Presumably, the F300W would be similar to the latter. We have increased the uncertainty I_{tot} to include these new estimates. The uncertainties in the EBL23 measurement are the combination in quadrature of the uncertainties in I_{DGL} discussed in § 2 and I_{ZL} and I_{tot} as summarized above. The revised results for I_{ZL}, I_{DGL}, and I_{EBL}, in each of the WFPC2 *U*, *V*, and *I* bands, are listed in Table 3.

5. DISCUSSION

The EBL23 results we obtain are roughly 1–2 σ detections and can be quoted as upper limits at the +2 σ values on their own. We combine these with the lower limits to EBL23 that we derived in BFM02a based on the flux from resolved sources as measured by "ensemble photometry." Our interpretation of the EBL, here as in BFM02c, is based on those upper and lower limits together.

5.1. *Number Counts and Luminosity Functions*

Provided that their photometry is accurate, the number counts are the simplest, most complete, and most accurate measurement available of the total starlight in the universe. Unfortunately, *any*

photometry of faint galaxies will miss a significant fraction of their light. By "faint" we mean any source found at the statistical detection limit (e.g., $10\sigma_{\rm sky}$) of any image. Using a technique which we called "ensemble photometry," we demonstrated in BFM02a that more than 50% of the total galaxy light is missing from these well-detected cores of faint galaxies simply because the majority of a galaxy's light will lie below the $1\sigma_{\rm sky}$ isophotal limit if its core is at the detection limit and those wings cannot be recovered directly on an object-by-object basis. We used the results of our ensemble photometry in V and I to derive aperture corrections to Kron-like magnitudes, such as measured with SExtractor (Bertin & Arnouts 1996). Our aperture corrections were obtained as a function of the central surface brightness of the source relative to the detection limit of the data for WFPC2. No assumptions were made about the profiles of the sources. We applied these aperture corrections to the source catalogs from the Hubble Deep Field (HDF; Williams et al. 1996) observed with WFPC2 to obtain corrected galaxy number counts to compare with EBL23. While the raw HDF number counts appear to have a shallower slope near the detection limit, the corrected number counts do not display this turnover. They obey the usual relationship between apparent magnitude and surface number density, $N \propto 10^{\alpha m}$, where N is the number of galaxies per magnitude per square degree, down to the detection limit of the data with $\alpha = 0.34 \pm 0.01$ and 0.33 ± 0.01 at $22 < m < 27.5$ AB mag at V and I, respectively. If one assumes that the slope of the number counts does not become *steeper* beyond those detection limits, then the integrated flux from sources at 23–38 AB mag is roughly 1 cgs in V and I. (The limit 38 AB mag corresponds to an $M_V = 10$ AB mag dwarf galaxy at $z \sim 4$.) This is a likely maximum value for the EBL from all objects fainter than 23 AB mag, as discussed in BFM02c.

Similar aperture corrections have since been derived by Benitez et al. (2004). Differences between the two sets of corrections are probably due to the distribution of surface brightness profiles assumed by Benitez et al. (2004) in their simulations, which are affected by the detection threshold of the data from which they are derived and would be most affected at the faintest surface brightnesses. The differences are reduced when Benitez et al. include a correction for incompleteness below the detection threshold, but we did not include a similar incompleteness correction in our work. Although we believe that the Benitez et al. corrections may be missing some flux due to local sky estimates and the adopted profiles, their aperture corrections are based on the ACS data and total aperture magnitudes, and can easily be applied to ACS photometry of the Ultra Deep Field (UDF),[8] which are the deepest counts now available.

The UDF number counts are shown in Figure 2, along with the corrected UDF counts based on the Benitez et al. (2004) aperture corrections without their incompleteness correction for undetected sources. With these aperture corrections, the slope of the counts is constant to within 1 or 2 mag of the detection limit, at which point the aperture corrections are strongly affected by the assumed profile of the sources and may be underestimated. Nevertheless, it does appear that a turnover is now visible in the b and r counts, although the redder UDF images may still be missing sources. As emphasized in BFM02c, the important point for our purposes is that even if the counts are incomplete, additional flux from sources fainter than $m \sim 29$ is $\lesssim 0.2$ cgs if the number counts continue to follow the slope of the $23 < m < 29$ counts. As we discuss further below, it is not realistic to suggest that any diffuse measurement of the EBL in the foreseeable future will be able to measure a surface brightness level of ± 0.2 cgs at optical wavelengths to test this extrapolation.

The total flux from sources in each band fainter than $m = 23$ AB mag is 0.6, 0.4, 0.3, and 0.4 cgs in b, v, i, and z. The total flux of galaxies in the HDF field measured by WFPC2 (BFM02a) or ACS (Benitez et al. 2004) is around 0.2 cgs higher than in the UDF total due to the higher density of galaxies in that field (cosmic variance). The minimum EBL23 values we obtain by ensemble photometry from our own *HST* images are given in Table 3 and described in BFM02a. From BFM02c, the total flux from galaxies at 15–23 AB mag is 0.3, 0.5, and 0.7 cgs at U, V, and I. The total EBL from resolved sources fainter than $m = 15$ AB mag is then around 1 cgs in all bands. The uncertainties due to cosmic variance are as large as or larger than would be expected from sources beyond the detection limit if their numbers are extrapolated at a constant slope.

Obviously, it is not possible to know if the slope of sources changes beyond the direct detection limit. The slope of sources fainter than $m_v = 29$ mag that would be required to make a meaningful contribution to the EBL was discussed exhaustively in BFM02c. We do not regard it as interesting to discuss hypothetical faint sources further here. As we also discussed in § 4 of BFM02c, it is also possible to extrapolate beyond the detection limit based on the detailed luminosity functions with redshift. Unfortunately, based on the luminosity functions available in 2001, we concluded that it was not possible to provide meaningful additional constraints in this way due to the systematic uncertainties in the luminosity functions and their evolution. Even with the dramatically improved constraints on the high-redshift luminosity functions that are now available (e.g., Yan & Windhorst 2004 and references therein), this is still the case given the very deep limit of the current counts.

5.2. *The Bolometric EBL*

Constraints on the cosmic star formation rate and stellar mass density are based on the bolometric EBL. The tightest constraints in the near- and mid-infrared come from the lower limits based on the integrated counts (e.g., Fazio et al. 2004; Dole et al. 2006; Thompson et al. 2007) and the upper limits based on the attenuation of gamma-ray photons from distant extragalactic sources (e.g., Dwek & Krennrich 2005; Aharonian et al. 2006; Stecker et al. 2006). Direct measurements attempting to remove the foregrounds have not yet led to strong constraints (see Hauser & Dwek 2001; Dwek et al. 2005 for recent reviews). The most significant uncertainties now seem to lie in the 20–100 μm wavelength range. To fill in that range, the bolometric EBL can be estimated from models of its spectral energy distribution. In BFM02c, we adopted a model of the EBL spectrum from Dwek et al. (1998), which was based on the spectral energy distribution of detectable galaxies as a function of redshift, combined with estimates of the dust extinction and reradiation. We scaled that model to obtain upper and lower limits for spectral energy distribution of the EBL over the range 0.1–1000 μm. The upper and lower limits are not just bounded by optical and near-IR lower and upper limits but were also constrained at the time by the DIRBE detections at 125 and 240 μm (Hauser et al. 1998) and now by the near-IR source counts and gamma-ray measurements. That model still compares well with the observational constraints. The uncertainty is due to both the scaling and the model being scaled, since the spectral energy distribution is not well constrained in the mid-infrared. Our estimates of the total EBL and the implications regarding the star formation history and metal mass density in the universe are not affected by the revisions to EBL23 discussed here.

[8] See http://www.stsci.edu/hst/udf.

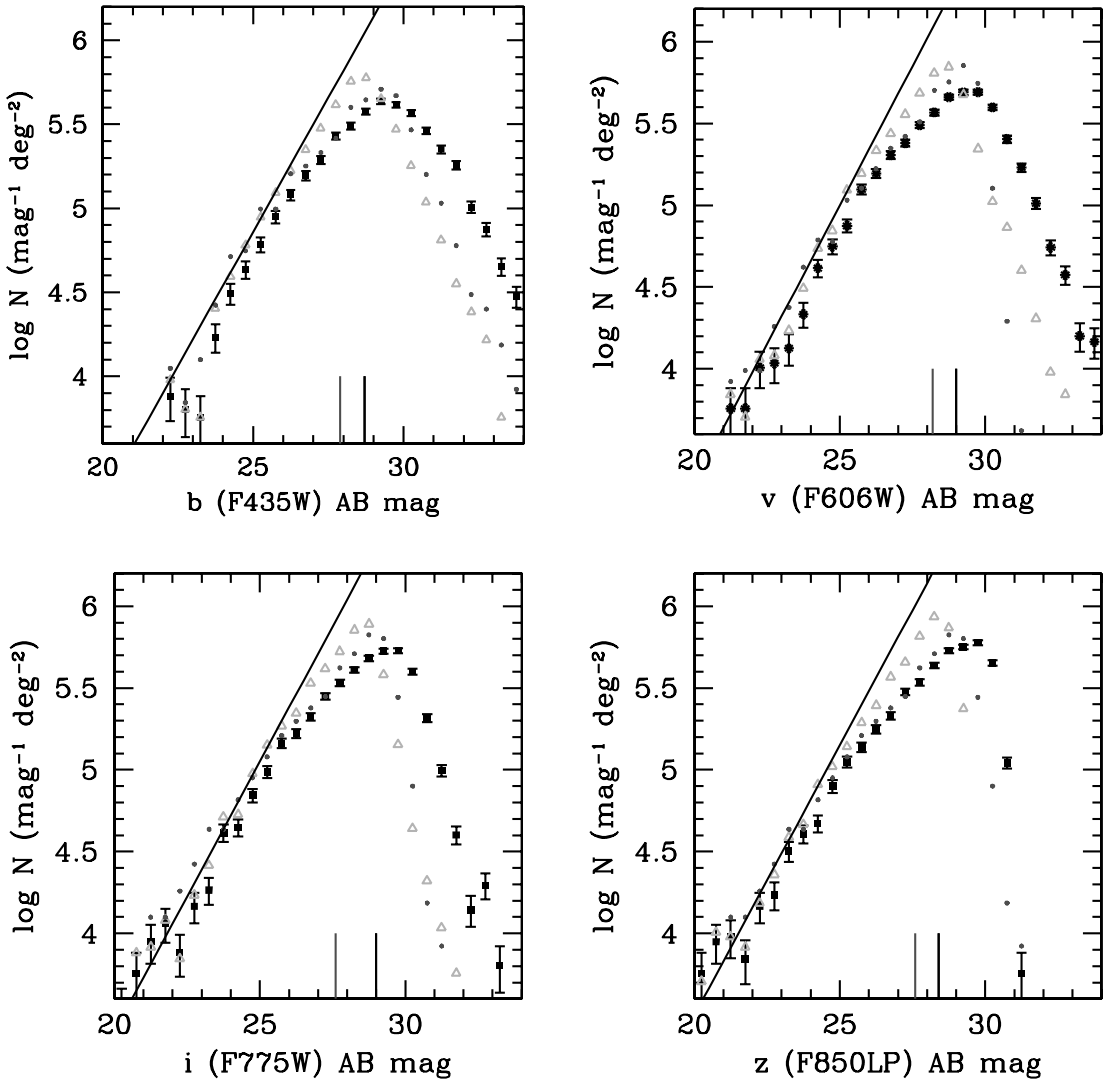

FIG. 2.—Total number of galaxies per magnitude per square degree in the UDF and HDF images. The Kron-like magnitudes in the UDF as measured by SExtractor using the GOODS detection parameters are shown by filled squares with $\sqrt{N}$ error bars. Open triangles show the same after applying the Benitez et al. (2004) aperture corrections for ACS data as a function of magnitude, without their correction for incompleteness. The small dots show the uncorrected, Kron-like magnitudes for the HDF field observed with WFPC2 (Williams et al. 1996). The straight lines in each plot show the relationship $N \propto 10^{\alpha m}$ with $\alpha = 0.32$, 0.34, 0.33, and 0.33 in *B* through *z* (see § 5 for discussion). The detection threshold for both data sets is shown by vertical lines at the bottom of the plots, with the UDF going deeper than the HDF in all bands. The variation in the density of sources at all apparent magnitudes is about 50% between these two fields with the HDF field being more dense. [*See the electronic edition of the Journal for a color version of this figure.*]

5.3. *Prospects for Future Measurements*

With regard to the nature of this experiment, it should be clear that the complexity of the corrections required to do absolute surface (spectro)photometry from the ground make it impossible to achieve 1% accuracy in the calibration of the ZL. As ~0.2% sensitivity would be required to make a more accurate measurement of the EBL than can be obtained from the resolved optical galaxy counts, the resolved galaxy counts do provide the best constraints. In general, the only promising strategy for isolating a diffuse source that has a surface brightness which is 1% of the diffuse foregrounds is to perform all measurements with the same instrument, so that the majority of corrections and foreground subtractions can be done in a relative sense, before the absolute calibration is applied. Note, however, that the foregrounds must be isolated spectroscopically (ZL) and spatially (foreground stars and bright galaxies) in the case of the EBL; it is much more difficult to achieve the required statistical and systematic accuracies in spectroscopy than in imaging, even from space. If the ZL were (nearly) removed from the problem by making a measurement beyond the zodiacal dust cloud (e.g., >3 AU from the Sun), the sky background might be dominated by DGL, ISL, and EBL, with a total flux toward the Galactic poles only several times brighter than the EBL. An instrument with a well-known PSF, several imaging filters, and a spatial resolution sufficient to remove nondiffuse Galactic sources might optimistically make a measurement of the EBL that was accurate to order 10%, or few × 0.1 cgs, which still might not conclusively constrain the slope of galaxies beyond the current detection limits.

6. SUMMARY

We have revised our EBL measurements based on changes to the absolute surface photometry of foreground sources in the field of our *HST* WFPC2 observations. The revised values are 6 ± 4, 10 ± 5, and 7 ± 4 cgs at *U*, *V*, and *I*, respectively. As the nominal results are only significant at the 1–2 σ level, as was true in BFM02a, the nominal results are clearly consistent with flux in integrated

sources, although the resolved sources themselves provide the most secure lower limit to the EBL. Moreover, as the total flux from resolved sources has largely converged at the detection limits of the deepest data, these lower limits are probably the most accurate estimate of the EBL available given the large foregrounds and therefore large uncertainties inherent in any absolute measurement of the EBL from the ground or with current technology from space. Given that the best sensitivities one can hope to achieve do not reach the $\ll 1$ cgs sensitivity levels that would provide interesting tests for extrapolations of resolve sources, more can be learned regarding the star formation history of the universe from the detailed study of the highest redshift sources directly than from the diffuse backgrounds at optical wavelengths.

To estimate the bolometric EBL, relevant to the total star formation history and metal production in the universe, the EBL must be constrained over 4 decades in wavelength, from the optical to the far-infrared. Models of the spectral energy distribution of resolved galaxies are required if one is to include the mid-IR EBL in this estimate. The models discussed in BFM02c are constrained by the resolved source lower limits and the near- and far-infrared observations, together, and are not affected by the revisions discussed here. Significant improvements in the estimate of the bolometric EBL will require better mid-IR constraints.

We thank M. Bershady, W. Freedman, B. Madore, K. Mattila, S. Shectman, and R. Windhorst for helpful comments on this work. The work presented in this paper is based on observations with the NASA/ESA *Hubble Space Telescope*, obtained by the Space Telescope Science Institute, which is operated by AURA, Inc., under NASA contract 5-26555. This research has made use of the NASA/IPAC Extragalactic Database (NED), which is operated by the Jet Propulsion Laboratory, Caltech, under contract to the National Aeronautics and Space Administration. Partial support for this work was provided by NASA through grants HF-01088.01-97A and GO-09066.08-A from STScI.

REFERENCES

Aharonian, F., et al. 2006, Nature, 440, 1018
Ashburn, E. V. 1954, J. Atmos. Terr. Phys., 5, 83
Beckers, J. 1995, in Scientific and Engineering Frontiers for 8–10 m Telescopes, ed. M. Iye & T. Nishimura (Tokyo: Tokyo Universal Acad.), 303
Beckers, J. M. 1993, ARA&A, 31, 13
Beichman, C. A., Neugebauer, G., Habing, H. J., Clegg, P. E., & Chester, T. J. 1986, *IRAS* Explanatory Supplement (Washington: GPO)
Bendix, J., Cermak, J., & Thies, B. 2004, in Proc. 3rd Int. Conf. on Fog, Fog Collection, and Dew, ed. H. Rautenbach & J. Olivier (Pretoria: Univ. Pretoria), http://www.up.ac.za/academic/geog/meteo/EVENTS/fogdew2003/PAPERS/C31.pdf
Benitez, N., et al. 2004, ApJS, 150, 1
Bernstein, R. A., Freedman, W. L., & Madore, B. F. 2002a, ApJ, 571, 56 (BFM02a)
———. 2002b, ApJ, 571, 85 (BFM02b)
———. 2002c, ApJ, 571, 107 (BFM02c)
———. 2005, ApJ, 632, 713 (BFM05)
Bertin, E., & Arnouts, S. 1996, A&AS, 117, 393
Burstein, D., & Heiles, C. 1982, AJ, 87, 1165 (BH82)
Capaccioli, M., & de Vaucouleurs, G. 1983, ApJS, 52, 465
de Vaucouleurs, G. 1958, ApJ, 128, 465
Dole, H., et al. 2006, A&A, 451, 417
Dwek, E., Arendt, R. G., & Krennrich, F. 2005, ApJ, 635, 784
Dwek, E., & Krennrich, F. 2005, ApJ, 618, 657
Dwek, E., et al. 1998, ApJ, 508, 106
Fazio, G. G., et al. 2004, ApJS, 154, 39
Gonzalez, A. H., Zabludoff, A. I., & Zaritsky, D. 2005, ApJ, 618, 195
Guhathakurta, P., & Tyson, J. A. 1989, ApJ, 346, 773
Hartmann, D., & Burton, W. B. 1997, Atlas of Galactic Neutral Hydrogen (Cambridge: Cambridge Univ. Press) (HB97)
Hauser, M. G., & Dwek, E. 2001, ARA&A, 39, 249
Hauser, M. G., et al. 1998, ApJ, 508, 25
Heyer, I., Richardson, M., Whitmore, B., & Lubin, L. 2004, Instrument Science Report WFPC2 2004-001 (Baltimore: STScI)
Holtzman, J., et al. 1995, PASP, 107, 156
Jura, M. 1979, ApJ, 227, 798
King, I. R. 1971, PASP, 83, 199
Kormandy, J. 1973, AJ, 78, 255
Krick, J. E., Bernstein, R. A., & Pimbblet, K. A. 2006, AJ, 131, 168
Leinert, C. et al. 1998, A&AS, 127, 1
Mackie, G. 1992, ApJ, 400, 65
Mattila, K. 2003, ApJ, 591, 119
McCartney, E. J. 1976, Scattering in the Atmosphere (New York: McGraw-Hill)
McClatchey, R. A., Fenn, R. W., Selby, J. E. A., Volz, F. E., & Garing, J. S. 1978, in Handbook of Optics, ed. W. G. Driscoll & W. Vaughan (New York: McGraw-Hill), 14-1
Middlemass, D., Clegg, R. E. S., & Walsh, J. R. 1989, MNRAS, 239, 5P
Racine, R. 1996, PASP, 108, 699
Savage, B. D., & Mathis, J. S. 1979, ARA&A, 17, 73
Schlegel, D. J., Finkbeiner, D. P., & Davis, M. 1998, ApJ, 500, 525 (SFD98)
Shectman, S. A. 1974, ApJ, 188, 233
Staude, H. J. 1975, A&A, 39, 325
Stecker, F. W., Malkan, M. A., & Scully, S. T. 2006, ApJ, 648, 774
Stover, J. C. 1990, Optical Scattering (New York: McGraw-Hill)
Surma, P., Seifert, W., & Bender, R. 1990, A&A, 238, 67
Thompson, R. I., Eisenstein, D., Fan, X., Rieke, M., & Kennicutt, R. C. 2007, ApJ, 657, 669
Toller, G. N. 1981, Ph.D. thesis, State Univ. New York
Uson, J. M., Boughn, S. P., & Kuhn, J. R. 1991, ApJ, 369, 46
Williams, R. E., et al. 1996, AJ, 112, 1335
Wolstencroft, R. D., & van Breda, I. G. 1967, ApJ, 147, 255
Yan, H., & Windhorst, R. A. 2004, ApJ, 612, L93